Hindawi
Advances in Civil Engineering
Volume 2024, Article ID 1448371, 12 pages
https://doi.org/10.1155/2024/1448371

Research Article

Stability Analysis of Soil and Rock Mixed Slope Based on Random Heterogeneous Structure

Yafei Wang,[1] **Zhanrong Zhang**,[1] **Xingpei Kang**,[1] **Hao Xie**,[1] **Chenchen Wang**,[2] **and Kun Liu**[2]

[1]*Chinese Railway Si-Yuan Survey and Design Group Co., Ltd., Wuhan, Hubei 430063, China*
[2]*School of Civil Engineering, Central South University, Changsha, Hunan 410075, China*

Correspondence should be addressed to Chenchen Wang; chenchenwang@csu.edu.cn

Received 7 March 2023; Revised 13 August 2023; Accepted 7 February 2024; Published 19 February 2024

Academic Editor: Antonello Troncone

Due to the complexity in the heterogeneous internal structure and interactions between rocks and soil, the slide of soil–rock mixed slope is usually more complex than that of a homogeneous soil slope. This paper investigated the stability of soil–rock mixed slopes with finite element method (FEM) based on random heterogeneous structure. An image-aided approach was used to generate the 2-D and 3-D digital rocks to ensure the morphology of digital rocks was similar with the real rocks. The 2-D and 3-D soil–rock mixed slopes were then generated by placing the digital rocks into the soil matrix. The generated heterogeneous structures of soil–rock mixed slope were imported into ABAQUS for numerical analysis. The effect of rock content, spatial distributions, material properties, and rock–soil interface on the stability of soil–rock mixed slopes were analyzed. Results show that the stability factor of the soil–rock mixed slope increases with the increase of rock content. The rocks can play a certain degree of antislide effect in the slope. The uneven spatial distribution of rocks has effect on the overall stability of soil–rock mixed slope. This effect is more significant when the rock content is moderate. Rocks distributed in the middle layer of the slope may improve the overall antisliding performance of the slope. The stability factor decreases with the increase of rock density. While the effect of rock elastic modulus on stability of soil–rock mixed slope is relatively limited. The contact condition at the soil–rock interface has effect on the overall stability of soil–rock mixed slope. It is recommended to properly determine the interface properties for stability analysis of soil–rock mixed slope.

1. Introduction

Soil–rock mixed slope is a geotechnical structure composed of discrete rocks and continuous soil matrix, which is different from bimrocks [1–3]. Bimrocks, denoting block-in-matrix rocks, encapsulate amalgamated rock masses comprising multiple lithological variations. The terrain under scrutiny manifests in this study as a heterogeneous geotechnical composite, characterized by a defined proportion of soil and boulders. In this context, the mechanical attributes of soil–rock mixed fill slopes, serving as composite structures comprising boulders and soil, are intrinsically influenced by the inherent attributes and spatial distribution of each constituent element. Due to the complexity in the heterogeneous internal structure and irregular external surfaces, the slide of soil–rock mixed slope is usually more complex than that of a homogeneous soil slope. Since the mechanical behavior of the soil–rock mixture cannot be accurately reflected through simply homogenization of soil and rocks, advanced modeling methods for soil–rock mixed slope with heterogeneous internal structure and irregular external surfaces are becoming a research hotspot in the field of slope stability analysis.

For the slope with irregular surfaces, the unmanned aerial vehicle three-dimensional (3-D) modeling technology combining UAV photography and 3-D modeling software can be well applied. The employment of UAVs as one of the GIS data sources is demonstrated by their capacity to provide precise 3-D models for GIS rendering [4]. UAV mapping is quick, dependable, precise, and economical. UAVs are effective for assessing slope dimensions and identifying potential slope risks based on the critical angle of the slope [5]. Congress et al. [6] employed UAV close-range photogrammetry (UAV-CRP) data

to assess highly weathered rock slopes near railroad tracks in Texas and built a framework for complete investigation of the stability of circularly damaged rocky slopes. Ghorbanzadeh et al. [7] achieved slope failure detection using a deep learning convolutional neural network in conjunction with an UAV for the region along the northern Himalayan part in India.

The internal structure also affects the stability of the slope. Some studies analyzed the soil–rock mixed fill as homogeneous material, which simplified the model and cut down on computation time, but ignored the heterogeneous structure of soil–rock mixed fill, which is not consistent with the actual situation [8–15]. Whereas geological exploration reveals that the existing civil engineering structures contain a significant amount of soil–rock mixed geology. It is necessary to study the stability of slopes under various soil–rock mixed conditions in order to provide guidance for excavation and reinforcement of soil–rock mixed slope projects [16, 17].

The digital image processing (DIP) is a commonly used technology to establish the structure model of soil–rock mixed slope. Huang et al. [18] obtained the appearance of the slope shear damage surface by computed tomography to assess the effect of rock distribution on slope stability. Since this modeling approach usually overlooks the actual distribution of blocks, the stochastic irregular block modeling technique becomes an alternative approach. In a numerical simulation analysis of particle discrete elements from a microscopic perspective, Chen et al. [19] investigated the differences between pure soil slopes and soil–rock mixed slopes in terms of stability, deformation bearing mechanism, and slip surface failure mechanism. Li et al. [20] used MATLAB code to produce random rock data with various groups of grain size, and they integrated it with other tools to create a finite difference model to examine how important factors like soil–rock interface strength affect the stability of soil–rock mixed slopes. The generated rock block shapes, however, did not completely match with the real rock block shapes in this process, and they are frequently simplified with regular shapes. Xu et al. [21] established a new polygonal block multicircle representation that can better simulate the mechanical properties and damage processes of rock blocks. Huang et al. [22] developed an elliptical block model by an improved stochastic algorithm and investigated the stability of the associated slopes. This demonstrates a more realistic rock mass shape and distribution is essential for the study of soil–rock mixed slopes.

Various studies used experimental techniques [23–26] and numerical simulation techniques [27, 28] to conduct stability analysis of soil–rock mixed slopes. Moreover, numerical analysis techniques have become more popular in slope stability analysis due to the quick development of computer technology and computational power. For nonhomogeneous structures like slopes made of soil and rock, material point method (MPM) [29–32] and the numerical manifold method (NMM) [33–39] are two of the popular numerical simulation techniques. MPM, a highly advanced numerical technique utilized by researchers, is specifically designed to simulate phenomena involving large deformations and fluid–solid interactions, enabling the analysis of damage processes. NMM, offers a unified framework for solving both continuous and discontinuous problems and finds extensive application in studying soil–rock mixed slopes. Additionally, the finite element method employed in this study is a well-established numerical method extensively employed in engineering. It effortlessly handles coupled problems in multiphysical fields and enhances computational efficiency by harnessing the parallel computing capabilities of modern computers. With its extensive functionalities and algorithms, it adeptly addresses complex structural and physical problems, yielding dependable outcomes. For both methods, accurate characterization of rock shape is important for model development. Therefore, this study contributes to the field by examining the stability of soil–rock mixed slopes using a random nonhomogeneous structure and the finite element method (FEM). The use of an image-aided approach to create realistic 2-D and 3-D digital rocks ensures accurate representation. By analyzing the impact of various factors on the stability of soil–rock mixed slopes, this study provides valuable insights that advance the current understanding of slope stability in geotechnical engineering.

2. Objectives

The primary objective of this study is to investigate the stability of soil–rock mixed slopes with finite element method (FEM) based on random nonhomogeneous structure. An image-aided approach was used to generate the 2-D and 3-D digital rocks to ensure the morphology of digital rocks were similar with the real rocks. The 2-D and 3-D soil–rock mixed slopes were then generated by placing the digital rocks into the soil matrix. The effect of rock content, spatial distributions, material properties, and rock–soil interface on the stability of soil–rock mixed slopes were analyzed.

3. Generation of Digital Soil–Rock Mixed Slope

3.1. Image-Aided Approach for Generating Digital Rocks. The soil–rock mixture is composed of discrete rocks and continuous soil matrix. Although the 3-D geometry of any single rock could be precisely reconstructed using X-ray CT technology, this technique is time-consuming and unsuitable for modeling in large quantities. Therefore, in this study, an image-aided approach was used to generate the 2-D and 3-D morphology of digital rocks. This approach not only considered the real shapes of the rocks but also introduce randomness in the algorithm. The generation process of digital rocks could be summarized as the following steps.

(1) Generating 2-D projections of rocks

The 2-D projections of rocks were captured in batches by using the aggregate image system (AIMS). In AIMS, the rocks with different sizes were placed on a round tray, which could rotate automatically. A fixed HD camera was used to capture the color images of the rocks on the tray one by one. The binary images (black and white) were then created from the color images. For each binary image, a series of points were generated along the black and white dividing line. These points were connected end-to-end to form a closed

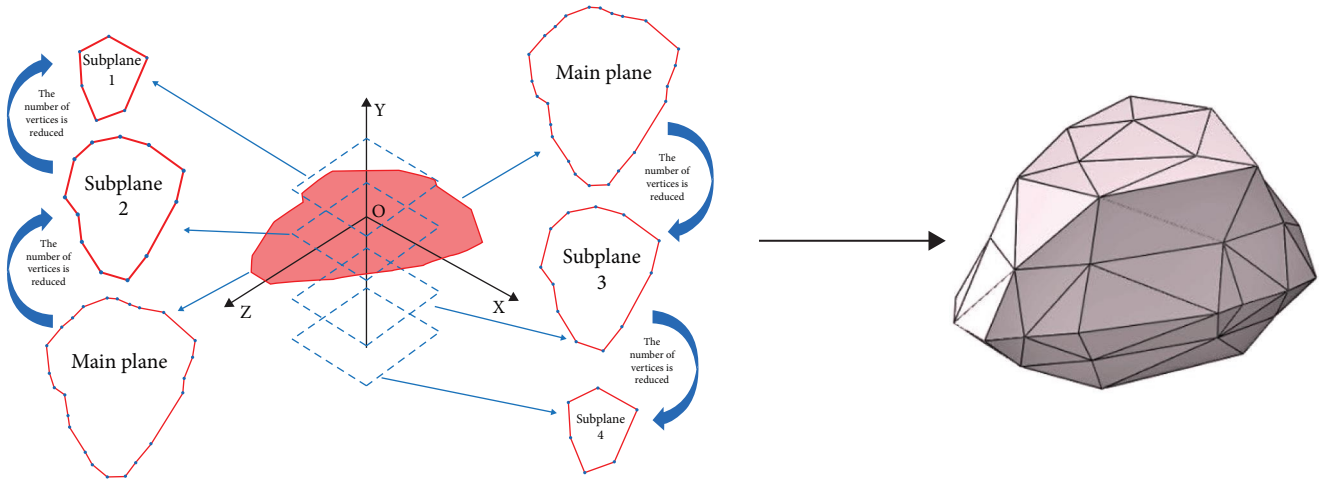

FIGURE 1: Schematic diagram of generating 3-D rocks.

polygon. This closed polygon could be used to represent a 2-D rock. However, to generate a 3-D digital rock, further processing was needed.

(2) Generating 3-D digital rocks with 2-D projections

Randomly select a 2-D polygon generated in the previous step, and place it in a 3-D Cartesian coordinate system shown in Figure 1. The centroid of the polygon should coincide with the origin of the coordinate system. This polygon is marked as main plane in Figure 1. Reduce the main plane to a certain scale, and then connect some of the vertices from end to end. Through the above method, a new polygon is generated and marked as Subplane 1 in Figure 1. Similarly, more polygons marked as Subplane 2, Subplane 3, and Subplane 4 are generated. Place these polygons in several planes parallel to the XOZ plane, and connect some specific vertices on any two adjacent polygons; a 3-D digital rock is generated. This 3-D rock is a polyhedron surrounded by several triangular meshes, as shown in Figure 1.

3.2. Generation of Random Irregular Slope Contours. The surface of the slope is usually uneven with irregular shape. Simplifying the slope surface to a regular plane may cause the analysis results to deviate from the real situation. The method for generating irregular surface of slope is divided into the following steps.

(1) Generation of slope with regular shape

A slope with regular shape was generated as shown in Figure 2(a). For the slope shown in Figure 2(a), only three surfaces were treated as exposed surfaces, and the other surfaces were set as boundaries. In other words, the irregularity was only considered for surface ABFE, surface BCOF, and surface CDGO. Some control points with specific spatial coordinates were generated along the edges of these three surfaces and were marked with blue color as shown in Figure 2(a).

(2) Generation of additional random points

A series of random points were generated above surface ABFE, surface BCOF, and surface CDGO. These additional points were marked with red color as shown in Figure 2(a).

(3) Generation of irregular surface

The irregular surfaces of the slope were generated by connecting the control points and additional points in a prescribed order. These irregular surfaces were represented by a series of triangular meshes, as shown in Figure 2(b).

3.3. Generation of Random Soil–Rock Mixed Slope with Irregular Contours. The method for generating random soil–rock mixed slope with irregular surfaces contains the following steps.

(1) Place a single rock in the slope

Randomly select a 3-D (or 2-D) rock generated in the previous sections. Assign random spatial coordinates to the centroid of the rock to place it into the slope.

(2) Assign spatial orientation to the rock

The spatial orientation of the rock inside the slope was adjusted with Equations (1)–(3). Equation (1) was used to rotate the rock around the x-axis α radian. Equation (2) was used to rotate the rock around the y-axis β radian. Equation (3) was used to rotate the rock around the z-axis γ radian.

$$\begin{aligned} y_n &= y_0 \cos\alpha - z_0 \sin\alpha \\ z_n &= y_0 \sin\alpha + z_0 \cos\alpha \\ x_n &= x_0, \end{aligned} \tag{1}$$

$$\begin{aligned} z_n &= z_0 \cos\beta - x_0 \sin\beta \\ x_n &= z_0 \sin\beta + x_0 \cos\beta \\ y_n &= x_0, \end{aligned} \tag{2}$$

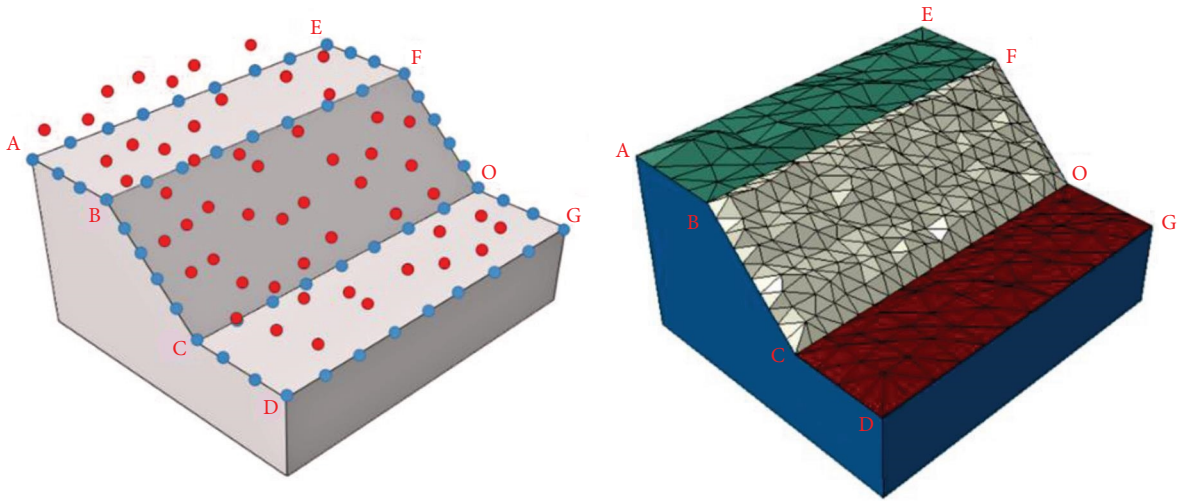

Figure 2: Schematic diagram of irregular slope surface modelling: (a) generation of random points above slope with regular shape and (b) 3-D slope with irregular surface.

$$\begin{aligned} x_n &= x_0 \cos\gamma - y_0 \sin\gamma \\ y_n &= x_0 \sin\gamma + y_0 \cos\gamma \\ z_n &= z_0, \end{aligned} \tag{3}$$

where x_0, x_n—x coordinate before and after rotation; y_0, y_n—y coordinate before and after rotation; z_0, z_n—z coordinate before and after rotation; α, β, γ—radians of rotation around x-axis, y-axis, z-axis.

(3) Check overlap between rocks and slope boundaries

The rocks should fall completely inside the slope, that is, any rock should not intersect with any boundary of the slope. If any rock overlapped with any boundary of the slope, a new spatial coordinate should be assigned to the rock until no overlap was observed.

(4) Check overlap between rocks

No overlap was allowed between any two rocks. If the current rock overlapped with any existing rock, a new spatial coordinate should be assigned to the rock until no overlap was observed.

(5) Integrate the discrete rocks with the slope

Boolean operation was applied to the rocks and slope after all the rocks were placed inside the slope. Then, the random soil–rock mixed slope with irregular contours was obtained, as shown in Figure 3. In Figure 3, some boundaries of the slope were hidden to show the internal structure. This soil–rock mixed slope model could be imported into commercial software ABAQUS for further analysis.

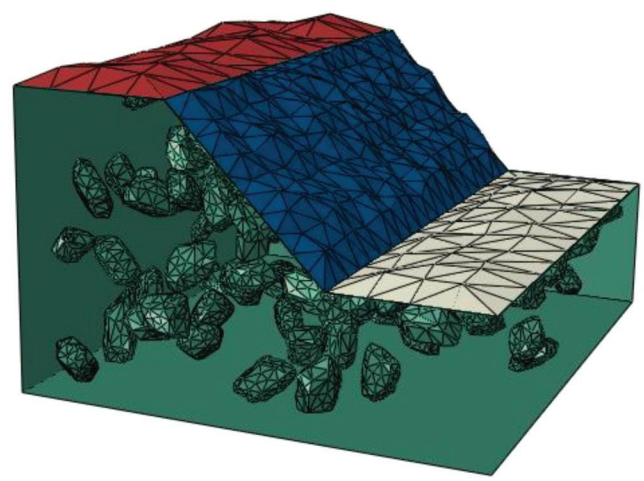

Figure 3: Examples of soil–rock mixed slope model.

4. Stability Analysis of Soil–Rock Mixed Slope

4.1. Finite Element Analysis of 3-D Soil–Rock Mixed Slope. A 3-D soil–rock mixed slope model was developed with the method described in the previous sections. The model size in the XOY plane was shown in Figure 4(a). The model size in the direction of Z-axis was 5 m. In this section, the irregularity of the slope surface was taken into consideration, while the primary focus was on the effect of nonhomogeneous structure on slope stability. The rock content of the soil–rock mixed slope was 5% in volume. The sizes of the rocks were randomly distributed from 1 to 2 m.

In order to ensure the mesh quality, the 3-D soil–rock mixed slope was meshed with tetrahedral elements and free meshing technique. A nonstandard interior element growth rate of 2.0 was applied to avoid excessive number of meshes inside rocks. Figures 4(b) and 4(c) show the meshes of the slope and the discrete rocks. Denser meshes could be observed around rocks. The material properties used in the finite element analysis are summarized in Table 1.

The strength reduction method was used to calculate the safety factor of the soil–rock mixed slope. The shear strength

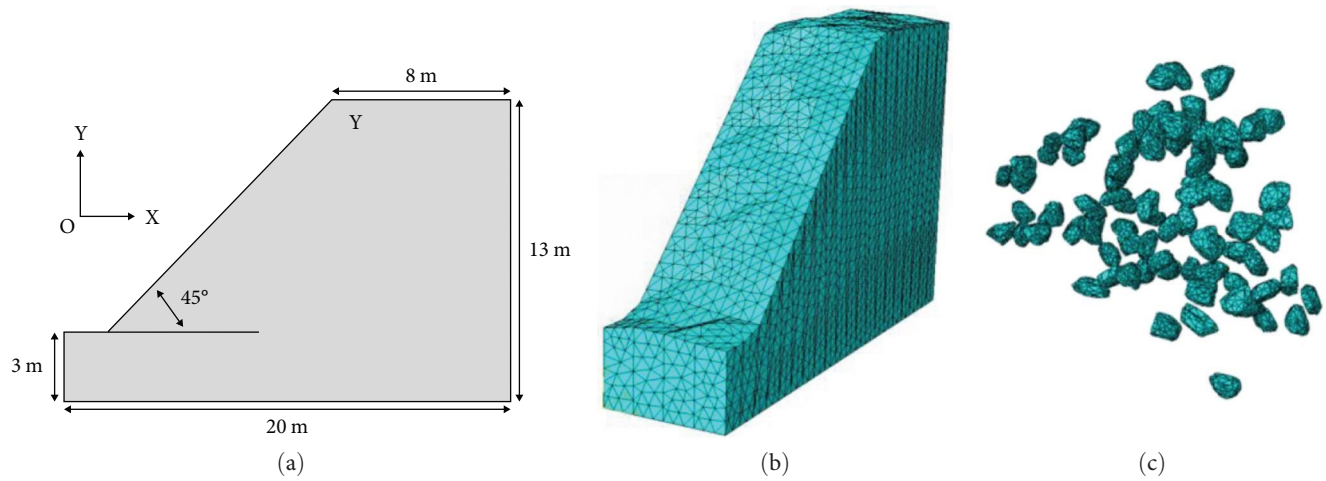

Figure 4: Finite element model of 3-D soil–rock mixed slope: (a) model size, (b) finite element meshes of slope, (c) finite element meshes of rocks.

Table 1: Material properties.

Material	Density (g/cm^3)	c' (kPa)	φ' (°)	E' (MPa)	ν'
Soil	2	12.38	20	100	0.35
Stones	2.5	—	—	400	0.3

parameters of the soil were expressed with Equations (4) and (5).

$$c_m = c'/F_r, \tag{4}$$

$$\varphi_m = \arctan(\tan \varphi'/F_r), \tag{5}$$

where c'—effective cohesion, φ'—angle of shearing resistance, c_m—reduced soil cohesion, φ_m—reduced friction angle, F_r—strength reduction factor.

In the finite element analysis, only the gravitational effects of soil and rocks were taken into consideration. It was assumed that there was tight contact between the rocks and the surrounding soil, with minimal relative slippage. When the shear strength of the soil reached a certain threshold, slope failure occurred. Figure 5 presents the displacement cloud diagrams of both the soil–rock mixed slope and a homogeneous soil slope. It is evident that the sliding surface of the homogeneous soil slope exhibits a more regular and smoother pattern, whereas the sliding surface of the soil–rock mixed slope appears to be uneven and more complex. This disparity can be attributed to the influence of randomly distributed rocks within the soil–rock mixed slope, which significantly affects the deformation characteristics of the entire slope.

To determine the impact of rock on slope deformation, the sections have been sliced to obtain internal displacement clouds. Considering the complex distribution of soil and rocks within the soil–rock mixed slope, a section is selected at intervals of 1.25 along the z-direction. Conversely, a homogeneous soil slope exhibits uniform internal structure, necessitating only one representative section positioned symmetrically to depict the entire slope, as depicted in Figures 5 and 6.

As can be seen from the figure, it is evident that the displacement within the soil–rock mixed slope is influenced by the distribution of stones, in contrast to the homogeneous soil slope. The presence of stones compels the soil to displace along the edges of the stones, resulting in a less smooth displacement cloud within the slope. This phenomenon adds complexity to the displacement deformation of the slope.

4.2. Finite Element Analysis of 2-D Soil–Rock Mixed Slope. Although the stability of the soil–rock mixed slope could be analyzed with the 3-D finite element model, the computational cost of the 3-D model is usually high. Alternatively, 2-D model could provide a more efficient way for investigating the stability of soil–rock mixed slope. In this section, a 2-D soil–rock mixed slope model was developed by placing 2-D digital rocks into the slope. The size of the 2-D soil–rock mixed slope model was the same with the cross section of the 3-D model, which was shown in Figure 4(a). Different rock contents ranging from 0%–50% were considered. To ensure the mesh quality, the 2-D soil–rock mixed slope models were meshed with triangular elements and free meshing technique. The material properties used in the 2-D models were the same with that used in the 3-D model, as shown in Table 1. Three-node linear 2-D plane strain elements are utilized for the stability analysis.

It is challenging to reconstruct a soil–rock mixed slope that is exactly the same with one in reality. Therefore, in order to validate the finite element model, the stability factor of the 2-D soil–rock mixed slope model with a rock content of zero was calculated, which was 1.053. While the stability factor of the soil slope with rock content of zero calculated through the limit equilibrium method is 1.0. That means the relative error of the presented model was about 5.3% when the rock content was zero.

5. Discussions

5.1. Effect of Rock Content on Slope Stability. In this section, a series of 2-D soil–rock mixed slope models with different

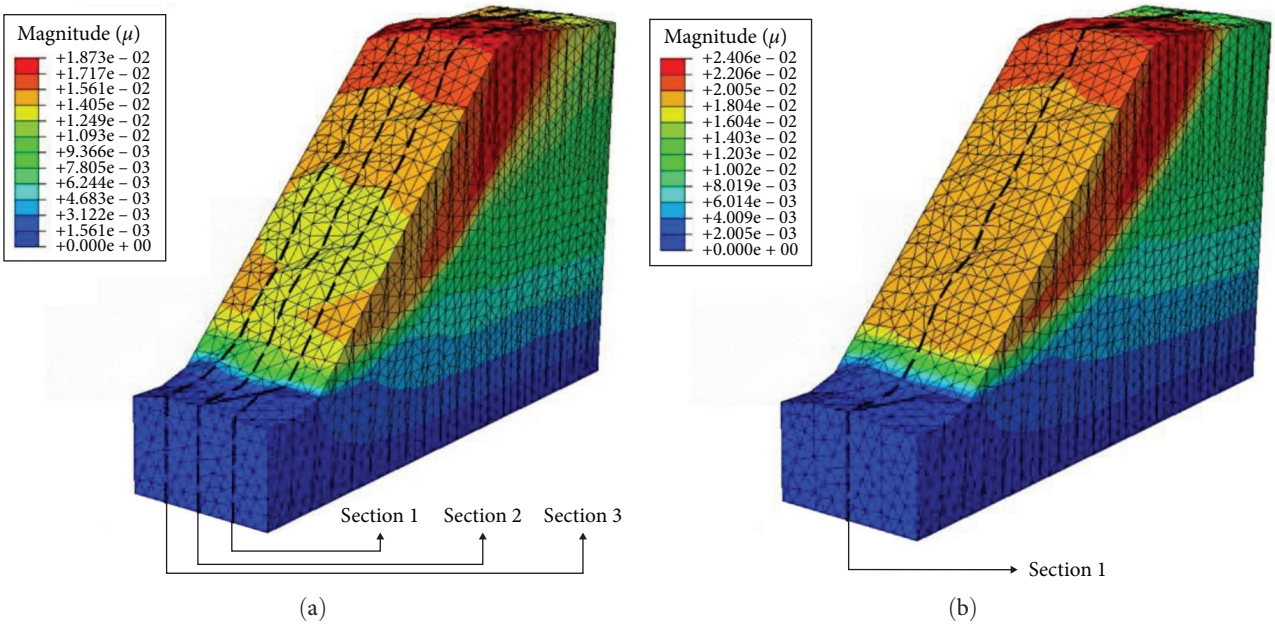

Figure 5: Displacement cloud diagrams of (a) soil–rock mixed slope and (b) homogeneous soil slope.

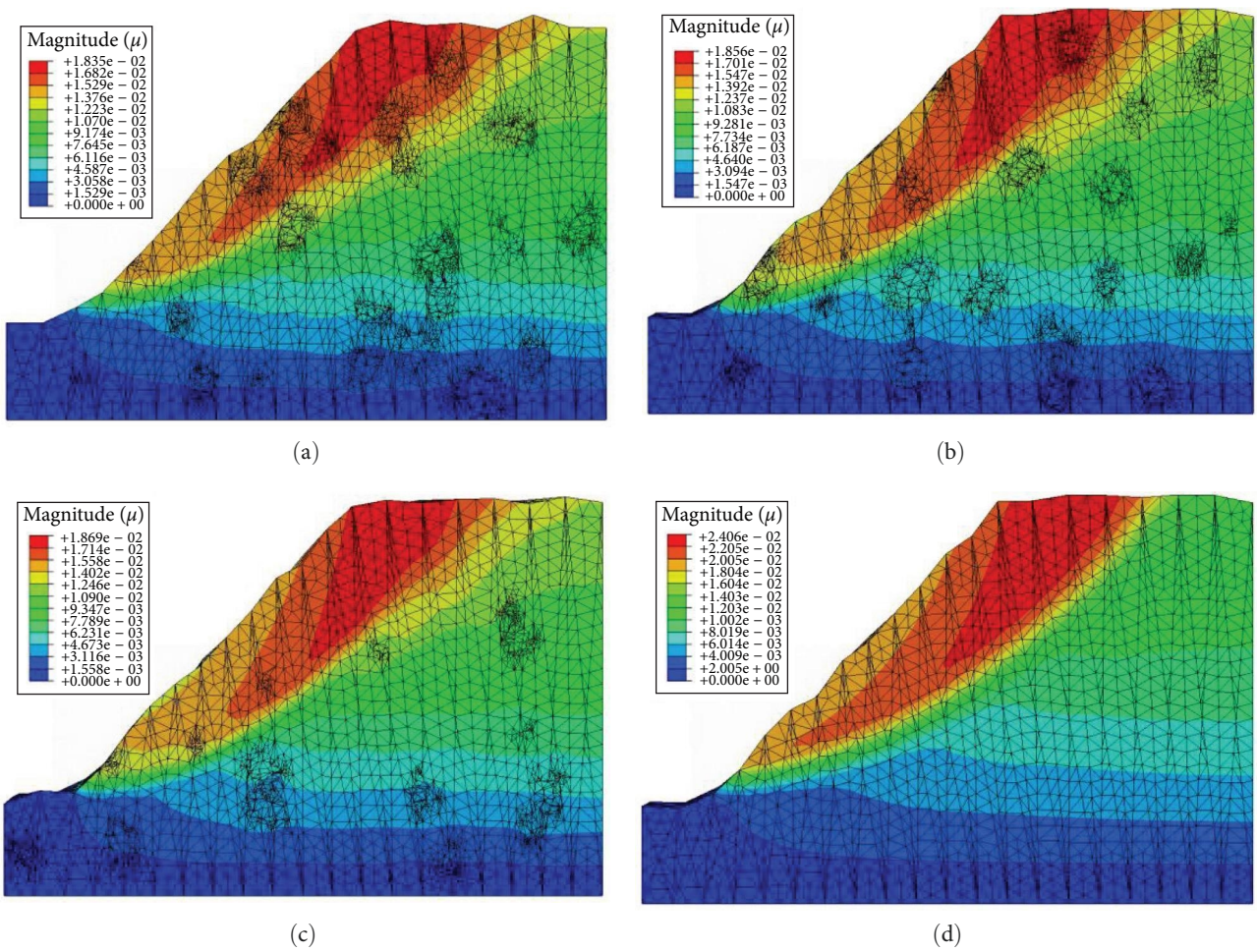

Figure 6: Internal slope displacement cloud diagrams: (a) mixed slope section 1, (b) mixed slope section 2, (c) mixed slope section 3, and (d) homogeneous soil slope section.

Table 2: Stability factor of soil–rock mixed slope with different rock contents.

Rock content (%)	Stability factors of different soil–rock mixed slope models					Average safety factor
	Model 1	Model 2	Model 3	Model 4	Model 5	
0	1.053	1.053	1.053	1.053	1.053	1.053
5	1.053	1.027	1.107	1.056	1.107	1.070
10	1.047	1.029	1.124	1.101	1.185	1.097
15	1.233	1.213	1.261	1.102	1.225	1.207
20	1.338	1.273	1.277	1.148	1.237	1.255
25	1.377	1.343	2.034	1.074	1.737	1.513
30	1.495	1.440	2.374	1.201	1.737	1.650
35	1.503	1.723	2.562	1.184	1.847	1.764
40	2.132	2.220	2.673	1.600	2.431	2.211
45	2.860	2.100	2.469	2.205	2.305	2.388
50	2.922	2.829	2.996	3.077	2.273	2.819

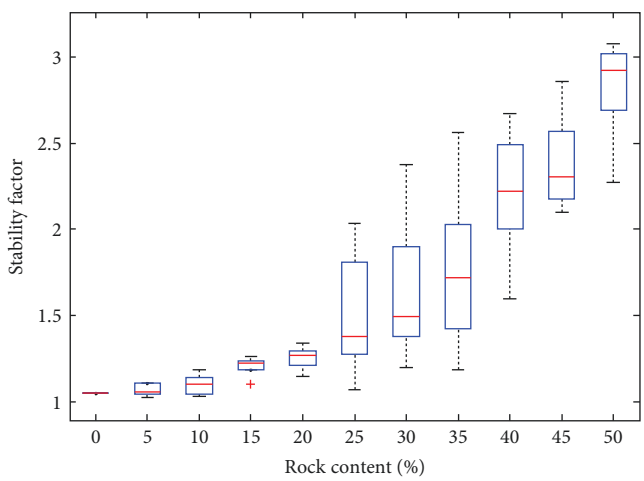

Figure 7: Stability factor of soil–rock mixed slope with different rock contents.

rock contents were generated to analyze the effect of rock content on the stability of slope. Totally 11 different rock contents ranging from 0% to 50% were considered. For each rock content, five models with different rock distributions were generated. To avoid the impact of excessive difference in rock size on the results, the rock sizes were uniformly distributed from 1.5 to 2.5 m for all models. The stability factor of each model was calculated, and the results are shown in Table 2.

It is observed that the stability factors of different models are different, even for the same rock content. For example, when the rock content is 25%, the minimum stability factor is 1.074 (Model 4), and the maximum stability factor is 2.034 (Model 3). The average stability factor of the five models is 1.513. This indicates that the rock distributions also affect the stability of soil–rock mixed slopes. In addition, Table 2 shows that the overall stability factor increases with higher rock content. This trend could be recognized more obviously with the boxplot shown in Figure 7. From the overall trend, the stability factor of the soil–rock mixed slope increases with the increase of rock content. This is mainly because the plastic deformation and plastic failure occur only inside the soil, not in the rocks. At the same time, since the elastic modulus and strength of the rock is much higher than the soil, the rocks can play a certain degree of antislide effect in the slope.

It should be noted that, as shown in Figure 7, when the rock content is relatively low (e.g., 0%–20%), the variation of stability factors calculated with different models is relatively small under the same rock content. When the rock content is moderate (e.g., 25%–40%), the variation of stability factors is relatively large under the same rock content. When the rock content is larger (e.g., 45%–50%), the variation of stability factors is smaller than that when the rock content is moderate. The main reason for this phenomenon is that, when the rock content is small, the effect of rocks on the overall slope stability is limited. When the rock content is too large, the rocks have been evenly distributed in different positions in the slope. In this case, even though the spatial distribution of each rock differs in different models, the overall distribution of rocks is relatively uniform in the slope. Only when the rock content is moderate, there may be obvious nonuniformity in the distribution of rocks in different models, which may lead to differences in the calculated stability factors.

5.2. Effect of Rock Spatial Distribution on Slope Stability. Previous results in Table 2 have indicated that the rock distributions may affect the stability of soil–rock mixed slopes. In order to further investigate the effect of rock spatial distribution on the slope stability, some soil–rock mixed slope models with some specific rock distributions were generated, as shown in Figure 8. In Figure 8(a)–8(c), the slopes were divided into horizontal layers, and the rocks were distributed in the upper layer, middle layer, and lower layer, respectively. The rock content in each layer shown in Figure 8(a)–8(c) was the same. In Figure 8(d)–8(f), the slopes were divided into vertical layers, and the rocks were distributed in the left layer, middle layer, and right layer, respectively. The rock content in each layer shown in Figure 8(d)–8(f) was the same. In Figure 8(g)–8(i), the slopes were divided into inclined layers, and the rocks were distributed in the upper layer, middle

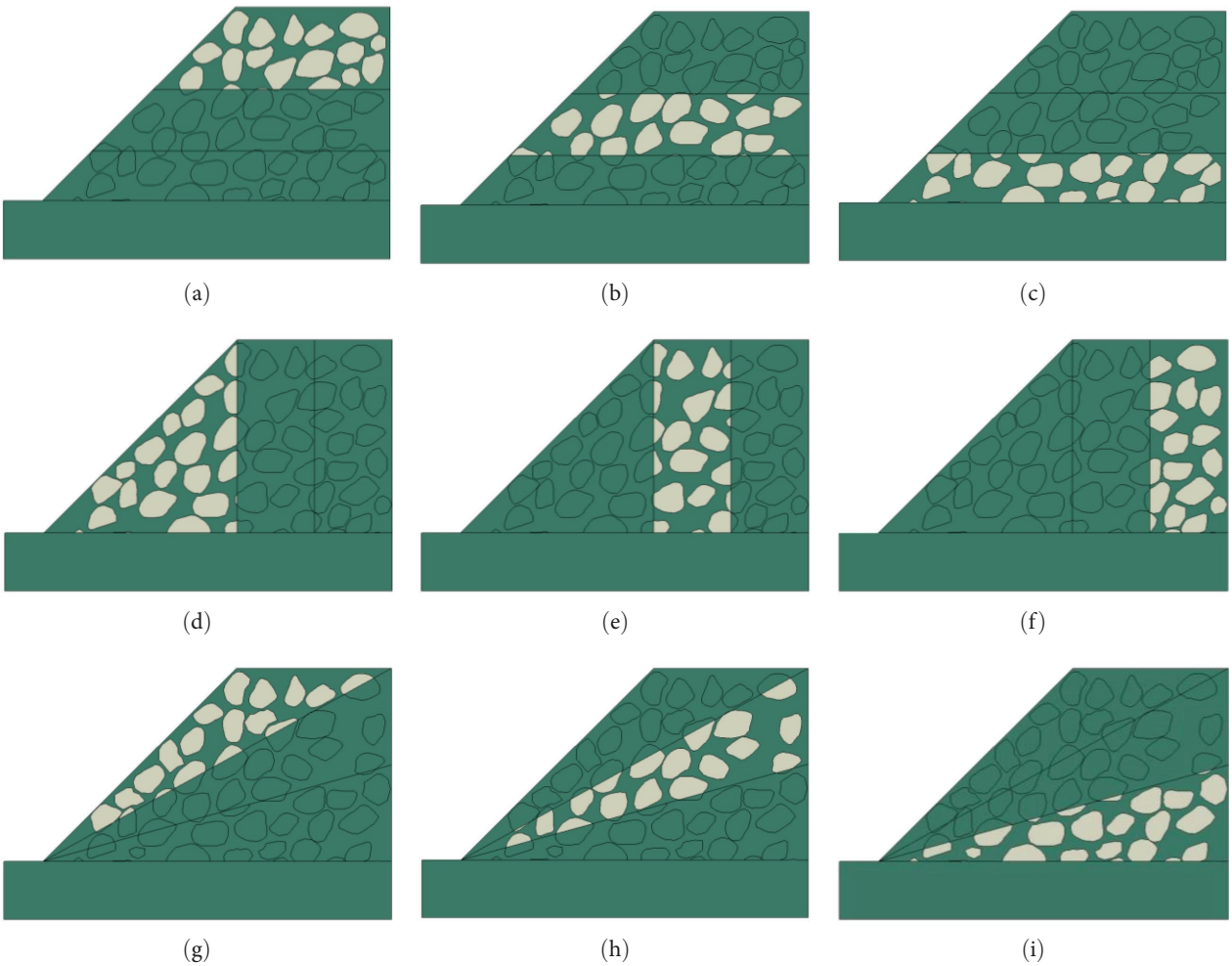

Figure 8: (a–i) Soil–rock mixed slope models with specific rock distributions.

layer, and lower layer, respectively. The rock content in each layer shown in Figure 8(g)–8(i) was the same.

The stability factors of different soil–rock mixed slope models shown in Figure 8 were calculated through finite element analysis, and the results are shown in Figure 9. Figure 9(a) shows the stability factors of slopes with horizontal layers. The minimum stability factor was observed when the rocks distributed in the horizontal upper layer, while the maximum stability factor was observed when the rocks distributed in the horizontal middle layer. One possible reason for this phenomenon is that the density of rocks is higher than that of the soil. When the rocks are concentrated in the upper layer, the rocks apply their gravity to the whole slope but cannot enhance the stability of the middle and lower layers. When the rocks are concentrated in the middle layer, the rocks only apply the gravity to the middle and lower layer and enhance the stability of the middle layer at the same time. When the rocks are concentrated in the lower layer, the rocks can neither apply gravity to the upper and middle layers, nor enhance stability of these layers.

Figure 9(b) shows the stability factors of slopes with vertical layers. The minimum stability factor was observed when the rocks distributed in the vertical right layer, while the maximum stability factor was observed when the rocks distributed in the vertical left layer. This is because, when the rocks are concentrated in the left layer, the stability of the left layer was enhanced. The improvement of antisliding performance in this layer will further prevent the sliding of the other two layers, thus significantly improving the overall antisliding performance of the slope. When the rocks are concentrated in the middle layer, these rocks improve the stability of the middle and right layers but have little effect on the stability of the left layers. Therefore, the stability factor in this case is still lower than that when the rocks distribute in the left layer.

Figure 9(c) shows the stability factors of slopes with inclined layers. It is observed that, when the rocks are concentrated in the inclined middle layer, the stability factor is the largest. One possible reason is that the inclined middle layer overlaps with the sliding surface of the homogeneous soil slope. In this case, the overall antisliding performance of the whole slope was improved.

Figure 9 also shows that the average stability factor of the horizontally layered slope is the largest, while the average stability factor of the slope with inclined layers is the smallest. This indicates the inclined layers discussed in this section are unfavorable to slope stability.

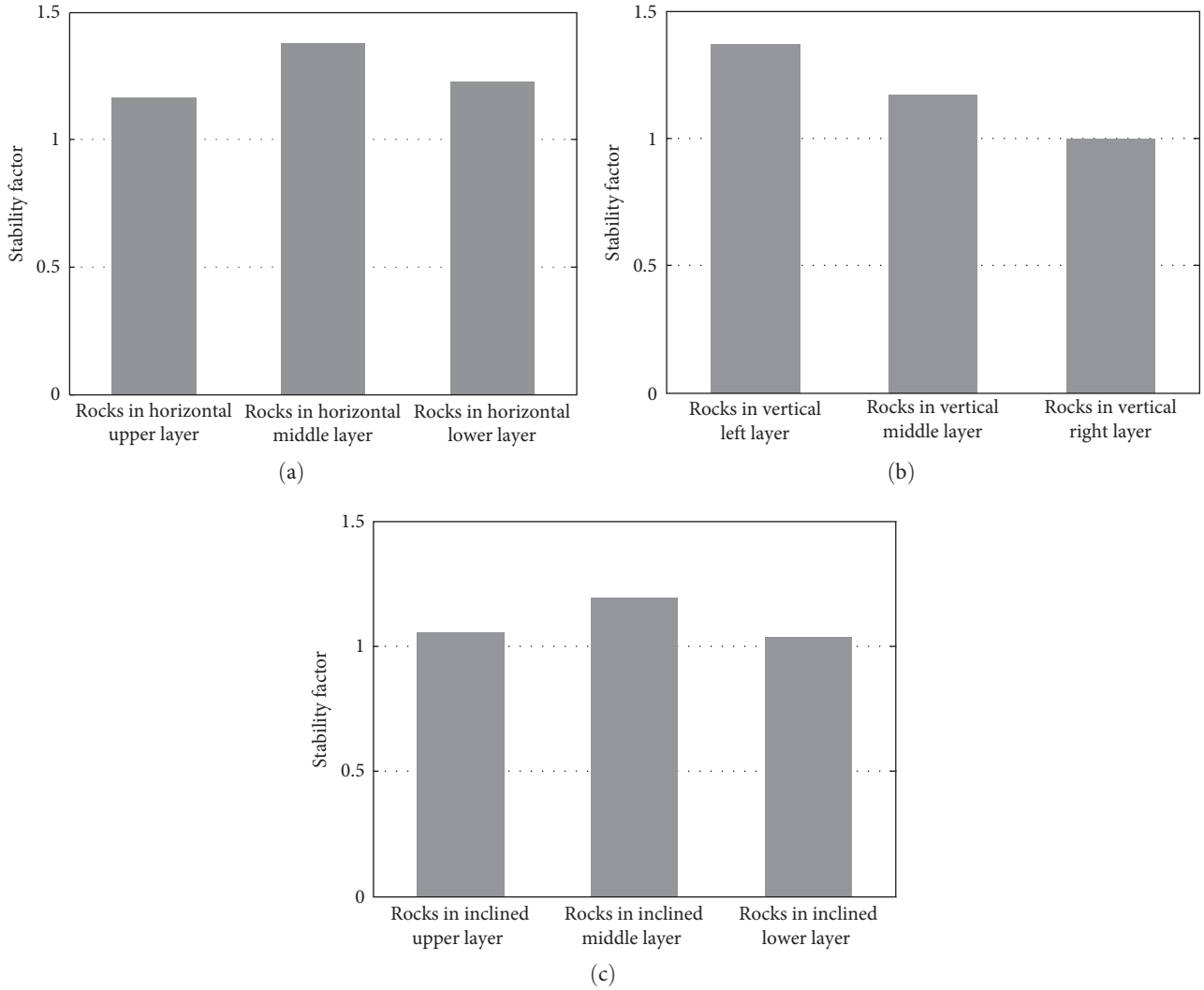

Figure 9: (a–c) Stability factor for slopes with specific rock distributions.

5.3. Effect of Material Properties on the Slope Stability. To investigate the effect of material properties on the slope stability, a 2-D soil–rock mixed slope model with rock content of 30% was generated. In the above model, the density of rock ranged from 1,000 to 3,000 kg/m^3, while the elastic modulus of rock ranged from 100 to 600 MPa. The other material properties were kept the same with that used in the previous sections. When analyzing the effect of rock density, the elastic modulus of rock was taken as 400 MPa. When analyzing the effect of rock elastic modulus, the density of rock was taken as 2,500 kg/m^3. The stability factors of the soil–rock mixed slope model with different material properties were calculated through finite element analysis, and the results are shown in Figure 10.

As shown in Figure 10(a), the stability factor decreases with the increase of rock density. This is understandable because higher density results in additional gravity. It is observed from Figure 10(b) that the effect of rock elastic modulus on stability of soil–rock mixed slope is relatively limited within the scope of the analysis in this section. One possible reason is that the elastic modulus of rock is usually much higher than the soil. As a result, the deformation of the soil–rock mixed slope is mainly due to the deformation of the soil. When the strength of the rock is adequate, the rocks in the soil–rock mixed slope could move with the deformation of the soil, but the elastic modulus of the rock has no obvious effect on the overall stability of the slope.

5.4. Effects of Soil–Rock Interface on the Stability of Soil–Rock Mixed Slope. The contact characteristics at the soil–rock interface would directly affect the stress transfer between soil and rock and may affect the deformation and stability of the slope. In order to investigate the effect of soil–rock interface on the stability of soil–rock mixed slope, a 2-D finite element model of soil–rock mixed slope was generated considering the following contact conditions:

(1) Full contact. In this condition, the rock tightly contacted with the surrounding soil with no tangential slip or normal separation at the soil–rock interface.

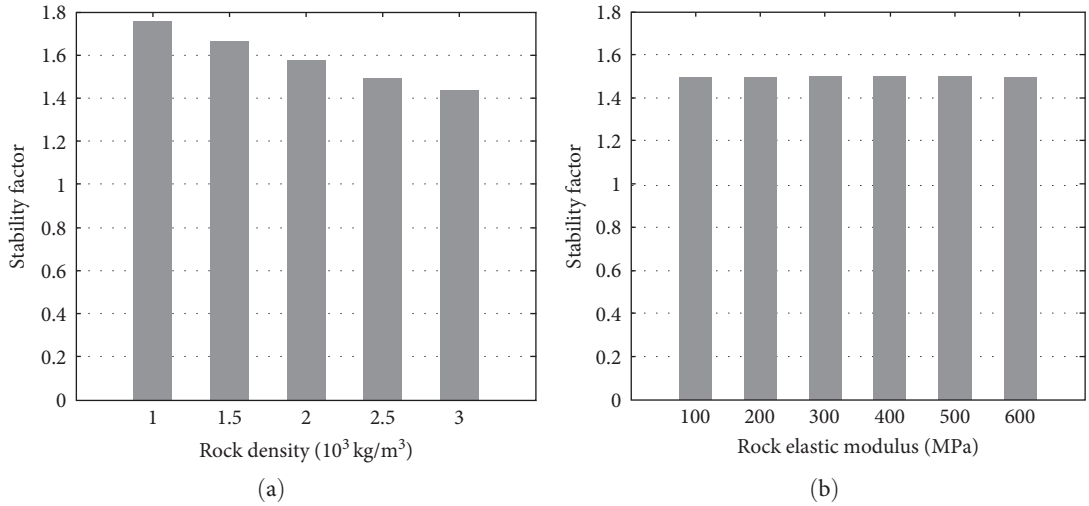

Figure 10: Variation of stability factor with (a) rock density and (b) rock elastic modulus.

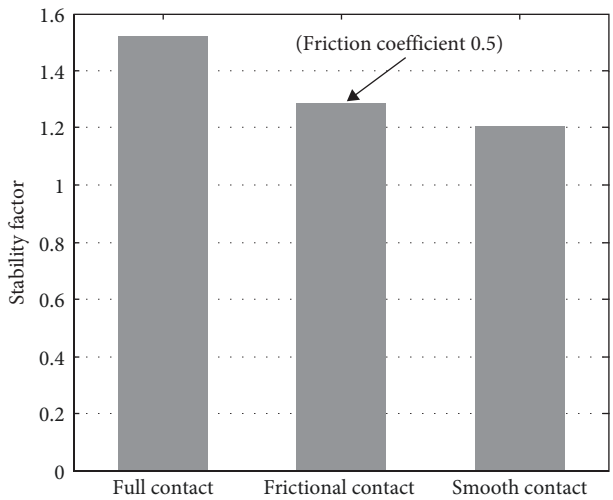

Figure 11: Effect of soil–rock interface on slope stability.

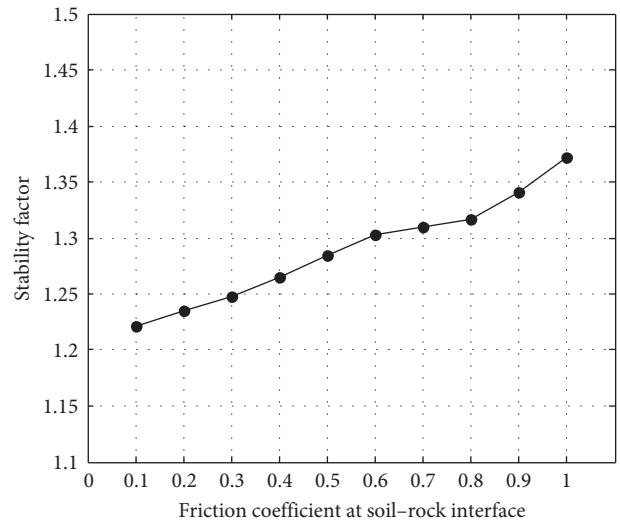

Figure 12: Effect of friction coefficient on slope stability.

(2) Frictional contact. In this condition, the tangential slip at the soil–rock interface was controlled by the friction coefficient. Normal separation between rock and soil was allowed at the soil–rock interface.

(3) Smooth contact. In this condition, the tangential slip at the soil–rock interface was allowed with no frictions. Normal separation between rock and soil were allowed at the soil–rock interface.

The stability factors for the above contact conditions were calculated with finite element method, and the results are shown in Figure 11. It is observed that the contact condition at the soil–rock interface has effect on the stability of the soil–rock mixed slope. The maximum stability factor is obtained under the full contact, while the minimum stability factor is obtained under the smooth contact. This indicates tighter contact at the soil–rock interface would improve the overall stability of the soil–rock mixed slope.

In Figure 11, the friction coefficient for the frictional contact condition was 0.5. To investigate the effect of friction coefficient on the slope stability, a series of friction coefficient ranging from 0.1 to 1.0 were used for finite element analysis. The calculated stability factors are summarized in Figure 12. It is observed that, when the friction coefficient increases from 0.1 to 1.0, the stability factor increases from 1.221 to 1.372. Since the contact condition at the soil–rock interface has effect on the overall stability of soil–rock mixed slope, it is recommended to properly determine the interface properties for related analysis, especially for the numerical analysis.

6. Conclusions

In this study, the stability of soil–rock mixed slopes was investigated with finite element method (FEM), based on random nonhomogeneous structures. An image-aided approach is employed to create 2-D and 3-D digital rocks that closely resemble real rocks. These digital rocks are then incorporated

into the soil matrix to form the 2-D and 3-D soil–rock mixed slopes. The effect of rock content, spatial distributions, material properties, and soil–rock interface on the stability of soil–rock mixed slopes was analyzed with 2-D. The following conclusions were obtained from the analysis:

(1) The stability factor of the soil–rock mixed slope increases with the increase of rock content. The rocks can play a certain degree of antislide effect in the slope.
(2) The uneven spatial distribution of rocks has effect on the overall stability of soil–rock mixed slope. This effect is more significant when the rock content is moderate (e.g., 25%–40%).
(3) Rocks distributed in the middle layer of the slope may improve the overall antisliding performance of the slope.
(4) The stability factor decreases with the increase of rock density. While the effect of rock elastic modulus on stability of soil–rock mixed slope is relatively limited.
(5) The contact condition at the soil–rock interface has effect on the overall stability of soil–rock mixed slope. It is recommended to properly determine the interface properties for stability analysis of soil–rock mixed slope.

Data Availability

Data will be made available on request.

Conflicts of Interest

The authors declare that they have no conflicts of interest.

Acknowledgments

The authors acknowledge the support provided by the Chinese Railway Si-Yuan Survey and Design Group (Grant No. 2020K045-1).

References

[1] E. Medley and R. E. Goodman, "Estimating the block volumetric proportions of melanges and similar block-in-matrix rocks (bimrocks)," in *Paper presented at the 1st North American Rock Mechanics Symposium*, Austin, Texas, June 1994.
[2] M. L. Napoli, M. Barbero, E. Ravera, and C. Scavia, "A stochastic approach to slope stability analysis in bimrocks," *International Journal of Rock Mechanics and Mining Sciences*, vol. 101, pp. 41–49, 2018.
[3] E. Khorasani, M. Amini, M. F. Hossaini, and E. Medley, "Evaluating the effects of the inclinations of rock blocks on the stability of bimrock slopes," *Geomechanics and Engineering*, vol. 17, no. 3, pp. 279–285, 2019.
[4] K. N. Tahar, "A new approach on slope data acquisition using unmanned aerial vehicle," *International Journal of Recent Research and Applied Studies*, vol. 13, no. 3, pp. 780–785, 2012.
[5] M. F. Zolkepli, M. F. Ishak, M. Y. M. Yunus et al., "Application of unmanned aerial vehicle (UAV) for slope mapping at Pahang Matriculation College, Malaysia," *Physics and Chemistry of the Earth, Parts A/B/C*, vol. 123, Article ID 103003, 2021.
[6] S. S. C. Congress, A. J. Puppala, P. Kumar, A. Banerjee, and U. Patil, "Methodology for resloping of rock slope using 3D models from UAV-CRP technology," *Journal of Geotechnical and Geoenvironmental Engineering*, vol. 147, no. 9, Article ID 05021005, 2021.
[7] O. Ghorbanzadeh, S. R. Meena, T. Blaschke, and J. Aryal, "UAV-based slope failure detection using deep-learning convolutional neural networks," *Remote Sensing*, vol. 11, no. 17, Article ID 2046, 2019.
[8] Y. Zhang, G. Chen, B. Wang, and L. Li, "An analytical method to evaluate the effect of a turning corner on 3D slope stability," *Computers and Geotechnics*, vol. 53, pp. 40–45, 2013.
[9] Y. Liu, Q. Dai, and Z. You, "Viscoelastic model for discrete element simulation of asphalt mixtures," *Journal of Engineering Mechanics*, vol. 135, no. 4, pp. 324–333, 2009.
[10] E. Masad and N. Somadevan, "Microstructural finite-element analysis of influence of localized strain distribution on asphalt mix properties," *Journal of Engineering Mechanics*, vol. 128, no. 10, pp. 1105–1114, 2002.
[11] A. T. Papagiannakis, A. Abbas, and E. Masad, "Micromechanical analysis of viscoelastic properties of asphalt concretes," *Transportation Research Record*, vol. 1789, no. 1, pp. 113–120, 2002.
[12] Z. You and Q. Dai, "Dynamic complex modulus predictions of hot-mix asphalt using a micromechanical-based finite element model," *Canadian Journal of Civil Engineering*, vol. 34, no. 12, pp. 1519–1528, 2007.
[13] Q. Dai and Z. You, "Micromechanical finite element framework for predicting viscoelastic properties of asphalt mixtures," *Materials and Structures*, vol. 41, pp. 1025–1037, 2008.
[14] Q. Dai, "Prediction of dynamic modulus and phase angle of stone-based composites using a micromechanical finite-element approach," *Journal of Materials in Civil Engineering*, vol. 22, no. 6, pp. 618–627, 2010.
[15] Q. Dai, M. H. Sadd, V. Parameswaran, and A. Shukla, "Prediction of damage behaviors in asphalt materials using a micromechanical finite-element model and image analysis," *Journal of Engineering Mechanics*, vol. 131, no. 7, pp. 668–677, 2005.
[16] S. Liu, X. Huang, A. Zhou, J. Hu, and W. Wang, "Soil–rock slope stability analysis by considering the nonuniformity of rocks," *Mathematical Problems in Engineering*, vol. 2018, Article ID 3121604, 15 pages, 2018.
[17] Y. Yang, G. Sun, H. Zheng, and Y. Qi, "Investigation of the sequential excavation of a soil–rock-mixture slope using the numerical manifold method," *Engineering Geology*, vol. 256, pp. 93–109, 2019.
[18] X. W. Huang, Z. S. Yao, B. H. Wang, A. Z. Zhou, and P. M. Jiang, "Soil–rock slope stability analysis under top loading considering the nonuniformity of rocks," *Advances in Civil Engineering*, vol. 2020, Article ID 9575307, 15 pages, 2020.
[19] X. Chen, S. Shi, and Y. Junxiong, "Effect of micro characteristics of soil–rock mixture slope on formation of sliding surface," *Journal of Engineering Geology*, vol. 28, no. 4, pp. 813–821, 2020.
[20] L. Li, Y. Li, L. Zhao et al., "Method for generating random soil–rock mixed slope and stability analysis," *Journal of Hunan University*, vol. 44, no. 7, pp. 170–178, 2017.

[21] W.-J. Xu, L.-M. Hu, and W. Gao, "Random generation of the meso-structure of a soil–rock mixture and its application in the study of the mechanical behavior in a landslide dam," *International Journal of Rock Mechanics and Mining Sciences*, vol. 86, pp. 166–178, 2016.

[22] X.-W. Huang, Z.-S. Yao, W. Wang, A.-Z. Zhou, and P. Jiang, "Stability analysis of soil–rock slope (SRS) with an improved stochastic method and physical models," *Environmental Earth Sciences*, vol. 80, Article ID 649, 2021.

[23] D. E. Daniel, R. M. Koerner, R. Bonaparte, R. E. Landreth, D. A. Carson, and H. B. Scranton, "Slope stability of geosynthetic clay liner test plots," *Journal of Geotechnical and Geoenvironmental Engineering*, vol. 124, no. 7, pp. 628–637, 1998.

[24] Y. Okui, A. Tokunaga, M. Shinji, and S. Mori, "New back analysis method of slope stability by using field measurements," *International Journal of Rock Mechanics and Mining Sciences*, vol. 34, no. 3-4, pp. 234.e1–234.e16, 1997.

[25] M. Ahmadi-Adli, N. K. Toker, and N. Huvaj, "Prediction of seepage and slope stability in a flume test and an experimental field case," *Procedia Earth and Planetary Science*, vol. 9, pp. 189–194, 2014.

[26] R. J. Chandler, "Back analysis techniques for slope stabilization works: a case record," *Géotechnique*, vol. 27, no. 4, pp. 479–495, 1977.

[27] Y. Yang, G. Sun, and H. Zheng, "Stability analysis of soil–rock-mixture slopes using the numerical manifold method," *Engineering Analysis with Boundary Elements*, vol. 109, pp. 153–160, 2019.

[28] G. Sun, S. Lin, H. Zheng, Y. Tan, and T. Sui, "The virtual element method strength reduction technique for the stability analysis of stony soil slopes," *Computers and Geotechnics*, vol. 119, Article ID 103349, 2020.

[29] A. Troncone, E. Conte, and L. Pugliese, "Analysis of the slope response to an increase in pore water pressure using the material point method," *Water*, vol. 11, no. 7, Article ID 1446, 2019.

[30] A. Troncone, L. Pugliese, A. Parise, and E. Conte, "A simple method to reduce mesh dependency in modelling landslides involving brittle soils," *Géotechnique Letters*, vol. 12, no. 3, pp. 167–173, 2022.

[31] L. Zhao, N. Qiao, D. Huang, S. Zuo, and Z. Zhang, "Numerical investigation of the failure mechanisms of soil–rock mixture slopes by material point method," *Computers and Geotechnics*, vol. 150, Article ID 104898, 2022.

[32] A. Troncone, L. Pugliese, A. Parise, and E. Conte, "Analysis of a landslide in sensitive clays using the material point method," *Geotechnical Research*, vol. 10, no. 2, pp. 67–77, 2023.

[33] Y. Yang, G. Sun, H. Zheng, and C. Yan, "An improved numerical manifold method with multiple layers of mathematical cover systems for the stability analysis of soil–rock-mixture slopes," *Engineering Geology*, vol. 264, Article ID 105373, 2020.

[34] Y. Yang, T. Chen, and H. Zheng, "Mathematical cover refinement of the numerical manifold method for the stability analysis of a soil–rock-mixture slope," *Engineering Analysis with Boundary Elements*, vol. 116, pp. 64–76, 2020.

[35] Y. Yang, D. Xu, F. Liu, and H. Zheng, "Modeling the entire progressive failure process of rock slopes using a strength-based criterion," *Computers and Geotechnics*, vol. 126, Article ID 103726, 2020.

[36] Y. Yang, Y. Xia, H. Zheng, and Z. Liu, "Investigation of rock slope stability using a 3D nonlinear strength-reduction numerical manifold method," *Engineering Geology*, vol. 292, Article ID 106285, 2021.

[37] Y. Yang, X. Tang, H. Zheng, Q. Liu, and L. He, "Three-dimensional fracture propagation with numerical manifold method," *Engineering Analysis with Boundary Elements*, vol. 72, pp. 65–77, 2016.

[38] Y. Yang, X. Tang, H. Zheng, Q. Liu, and Z. Liu, "Hydraulic fracturing modeling using the enriched numerical manifold method," *Applied Mathematical Modelling*, vol. 53, pp. 462–486, 2018.

[39] Y. Yang, T. Chen, W. Wu, and H. Zheng, "Modelling the stability of a soil–rock-mixture slope based on the digital image technology and strength reduction numerical manifold method," *Engineering Analysis with Boundary Elements*, vol. 126, pp. 45–54, 2021.